Robust, bistable patterning of the dorsal surface of the *Drosophila* embryo

David M. Umulis*, Mihaela Serpe[†‡], Michael B. O'Connor[†‡§], and Hans G. Othmer[§¶]

Departments of *Chemical Engineering and Materials Science and [†]Genetics, Cell Biology, and Development, [‡]Howard Hughes Medical Institute, and [¶]School of Mathematics and Digital Technology Center, University of Minnesota, Minneapolis, MN 55455

Edited by Kathryn V. Anderson, Sloan–Kettering Institute, New York, NY, and approved June 19, 2006 (received for review December 2, 2005)

In many developing systems, the fate of a cell is determined by its position in a time-independent spatial distribution of a morphogen. However, during dorsal–ventral patterning in the *Drosophila* embryo, an initial low-level signal refines to a narrow, high-intensity band. This refinement suggests that cells respond to the local transient morphogen distribution that results from interactions between bone morphogenetic proteins (BMPs), their receptors, the BMP-binding proteins Sog and Tsg, the metalloprotease Tld, and a putative, positively regulated component that locally enhances surface binding of BMPs within the region of high signaling. We develop a computational model for dorsal surface patterning and show that, when positive feedback of a cell surface BMP-binding protein is incorporated, bistability in the kinetic interactions transduces the transient BMP distribution into a switch-like spatial distribution of the BMP-bound receptor. We also show that the inclusion of positive feedback leads to the observed contraction of signaling, because cells near the dorsal midline outcompete adjacent lateral cells for limited amounts of BMP. In the model, cells interpret the morphogen distribution by differentiating according to the history of their exposure rather than to a threshold concentration in a static spatial gradient of the morphogen.

mathematical model | morphogen | robustness | positive feedback

Patterning of the dorsal surface of the *Drosophila* embryo is mediated by a heterodimer of the bone morphogenetic proteins (BMPs) Decapentaplegic (Dpp) and Screw (Scw) (1–3). High concentrations of the heterodimer Dpp/Scw specify the presumptive amnioserosa along the dorsal midline (DM), whereas lower levels of Dpp/Scw along with Dpp and Scw homodimers specify the lateral dorsal ectoderm (1, 4, 5). Dpp/Scw signals through a heteromeric complex comprising Punt, a type II receptor, and two type I receptors, Thick veins (Tkv) and Saxophone (Sax) (6–8). BMP-occupied receptors (BRs) phosphorylate Mad to produce phosphorylated Mad (pMad), which binds to Medea and translocates to the nucleus, where it regulates the transcription of target genes.

The transient evolution of extracellular Dpp/Scw is controlled by intra- and extracellular processes that interact to produce a spatial pattern of pMad signaling that is initially broad but later refines to form a peak near the DM (Fig. 1 *a* and *b*) (9). Hereafter we use "intracellular" to refer to the syncytium, and we use "extracellular" to denote the perivitelline (PV) space. The extracellular Dpp/Scw distribution is modulated by interactions of Dpp/Scw with Short gastrulation (Sog) (10, 11), Twisted gastrulation (Tsg) (12, 13), and Tolloid (Tld) (14, 15). Sog and Tsg are BMP-binding proteins that form a high-affinity complex for the Dpp/Scw heterodimer (1), whereas Tld is a metalloprotease that cleaves Sog only when bound to ligand. Dpp/Scw, Tsg, and Tld are all broadly expressed within the dorsal domain, whereas Sog is produced in the adjacent ventral/lateral neuroectoderm regions. Sog levels are high near the interface between the ventral/lateral and dorsal domains, and in this region most Dpp/Scw is bound to Sog/Tsg and therefore unable to bind to receptors (16). The Dpp/Scw/Sog/Tsg complex is free to diffuse, which produces a flux toward the DM. Sog bound to Tsg and Dpp/Scw is cleaved by Tld, which releases Dpp/Scw. Free Dpp/Scw can then either bind to a receptor or rebind to another Sog/Tsg complex. Where Sog is high, the latter dominates, whereas where Sog is low, receptor binding dominates. In qualitative terms, localization of Dpp/Scw, and hence gene expression, at the DM results from a complex balance between diffusion of Dpp/Scw away from the midline, diffusion of Dpp/Scw/Sog/Tsg toward the midline, binding of Dpp/Scw to Sog/Tsg, release of Dpp/Scw from Sog/Tsg by Tld, and receptor binding (Fig. 1*c*).

Previous models focus on extracellular processes, incorporate a BMP-shuttling mechanism based on Sog, with or without Tsg, and predict accumulation of BMP and increased BRs near the DM (16, 17). Both models achieve localization of BMP at the DM by limiting the range of BMP diffusion after its release from a complex, either by setting the diffusion coefficient of free BMP to 0 (model I) (17) or by removing free BMP through rapid receptor-mediated turnover (model II) (16) (see *Supporting Materials*, section 4.3, which is published as supporting information on the PNAS web site). These models also address robustness and other aspects of patterning but do not incorporate the recent observation that dorsal surface patterning relies on a positive feedback mechanism that enhances BMP-receptor interactions (9). In addition, in the early embryo, BMP levels are low, and pMad signaling is weak, but as time progresses, pMad expression increases and the region of pMad expression contracts spatially, concentrating at the DM (Fig. 1 *a* and *b*). Neither model as given can reproduce this observation without artificially terminating the production of Dpp, but as we show later, this contraction occurs automatically with the inclusion of positive feedback.

It was shown previously that heterodimer formation (1), in conjunction with extracellular transport (16, 17), confers significant robustness to the morphogen distribution under changes in gene expression and parameter variations (18), and here we show that the addition of the positive feedback module that explains the transient evolution retains or enhances the robustness. The specific identity of the molecule involved in the positive feedback is not known, but we hypothesize, by analogy to posterior cross-vein development (18), that positive feedback involves induction of a cell surface-bound BMP-binding protein (SBP) such as Cv-2 (18) (Fig. 1*d*). Further support for this hypothesis derives from the fact that zebrafish gastrulation requires BMP-induced positive feedback of Cv-2, which exists in both a surface-bound form and a processed form that may be secreted (19). Positive feedback enhances BMP–receptor interactions and thus potentiates signaling in regions that have been previously exposed to the ligand (9).

Conflict of interest statement: No conflicts declared.

This paper was submitted directly (Track II) to the PNAS office.

Abbreviations: BMP, bone morphogenetic protein; BR, BMP-occupied receptor; DM, dorsal midline; PV, perivitelline; SBP, surface-bound BMP-binding protein.

[§]To whom correspondence may be addressed. E-mail: moconnor@mail.med.umn.edu or othmer@math.umn.edu.

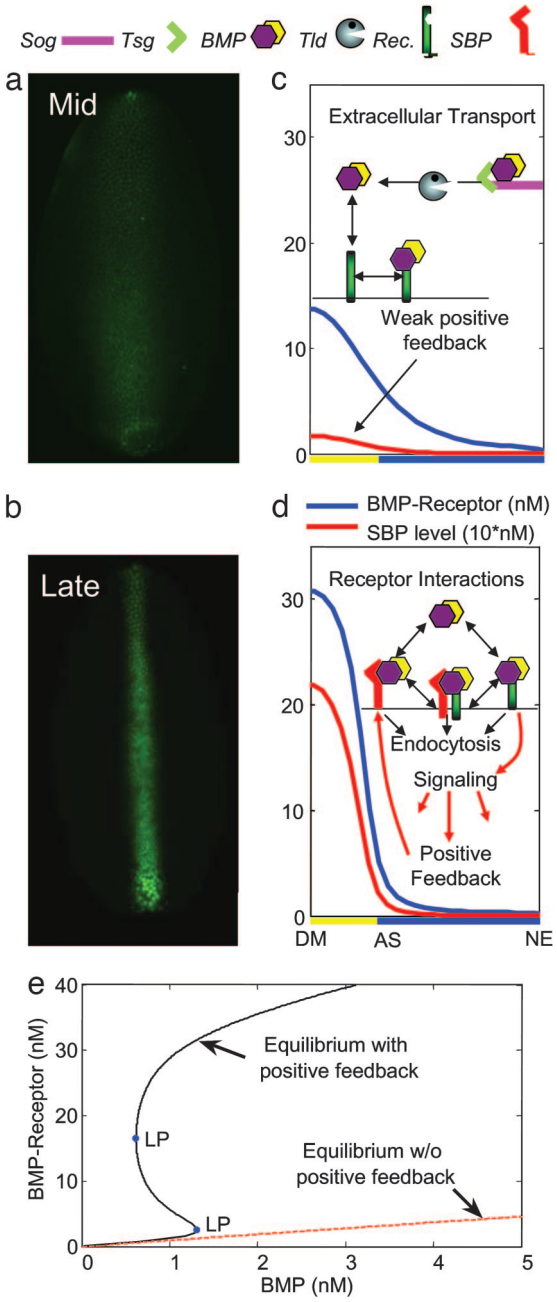

Fig. 1. Gene expression patterns and schematics of the model. Dorsal surface patterning assayed by the pMad staining evolves from a broad signaling profile (*a*) to a narrow, high-intensity profile (*b*). (*c*) Extracellular shuttling of Dpp/Scw by Sog/Tsg redistributes Dpp/Scw toward the DM. (*d*) Positive feedback via SBP enhances receptor–BMP interactions and focuses signaling in regions of previous high signaling. (For a more detailed figure, see Fig. 11 in *Supporting Materials*.) Plots show model results for 30 (*c*) and 60 (*d*) min. AS, amnioserosa; NE, neuroectoderm. (*e*) The steady-state response, as measured by the level of BR as a function of extracellular BMP, treated as a parameter. For low BMP, BR interactions closely follow the equilibrium-binding curve. When the level of extracellular BMP exceeds the lower limit point (LP) (blue dot), the lower branch disappears and the level of BR follows the upper branch. Once on the upper branch, the level of BR remains there until BMP drops below the level corresponding to the larger (in the BR) limit point, whereupon it drops to the lower branch.

The Model

It has been suggested that positive feedback coupled with a graded distribution of a morphogen can produce spatial bistability in embryonic patterning (9), which here means that for certain ranges of the morphogen concentration there are two alternative stable steady-states accessible to cells, and which one they adopt depends on the history of their morphogen exposure. As a result, there is hysteresis in the response to the morphogen level, because the switching point between these states will depend on whether the level is increased or decreased. Earlier analysis of hedgehog/patched (20) suggested that positive feedback by up-regulation of receptors can lead to spatial bistability in the level of bound receptors, and although this may be applicable in some systems, it is probably not the mechanism at work here (9). First, misexpression of Tkv in the embryo either does not significantly affect the output pMad signaling or in some cases leads to a reduction of BMP signaling, and, second, BMP receptors in other contexts are down-regulated, not up-regulated, in response to pMad signaling (9, 21). Furthermore, *tkv* zygotic mutants exhibit a normal signaling profile, which suggests that the feedback does not take place at the transcriptional control of receptors (see *Supporting Materials*, section 7.2). We consider positive feedback through up-regulation of a membrane/SBP coupled with endocytic removal of BMP from the PV space. In the *Supporting Materials* (section 4) we address and compare three other mechanisms: case 1, receptor binding with extracellular BMP decay; case 2, receptor-mediated endocytosis (16); and case 3, positive feedback with only extracellular decay.

A simplified mechanism for SBP action is shown schematically in Fig. 1*d*, and the complete mechanism with associated forward and reverse rates is included in *Supporting Materials* (Figs. 6 and 11 in *Supporting Materials*). BMP in the PV space can bind to either the receptor or the SBP, and in the latter case, this can increase the local concentration of BMP seen by the receptors. To function effectively the on- and off-rates must be suitably tuned; if the binding to SBP is too tight, then the protein simply sequesters the ligand and decreases the concentration seen by the receptor, whereas too low an affinity will lead to little or no effect of the protein (*Supporting Materials*, section 7.2). Because BMPs are dimers, we assume that BMP bound to the SBP through one monomer of the dimer leaves the other half exposed to the receptor. Thus the SBP/BR complex is bridged by the dimeric BMP, and release of the SBP leaves BMP bound to the receptor. Because signaling by TGF-β receptors requires recruitment of additional cofactors/receptors (type II receptor Punt, for instance), we assume that only BRs that are not bound to the SBP are signaling competent.

The evolution equations for components involved in the positive feedback loop are as follows; equations for other components are given in *Supporting Materials* (sections 1 and 2).

$$Dpp/Scw\ (\text{ext.}):\quad \frac{\partial B}{\partial t} = D_B \frac{\partial^2 B}{\partial x^2} + \gamma_1 \frac{V_{in}}{V_{PV}} \overline{DW_{in}} - k_3 I{\cdot}B + k_{-3} IB - k_4 B{\cdot}C + k_{-4} BC - k_5 B{\cdot}R + k_{-5} BR + \lambda Tol{\cdot}IB \quad [1]$$

$$\text{SBP}:\quad \frac{dC}{dt} = \frac{\Lambda{\cdot}BR^{\nu}}{K_h{}^{\nu} + BR^{\nu}}(t-\tau) - k_4 B{\cdot}C + k_{-4} BC - k_7 BR{\cdot}C + k_{-7} BCR - \delta_E C \quad [2]$$

$$Dpp/Scw/\text{SBP}:\quad \frac{dBC}{dt} = k_4 B{\cdot}C - k_{-4} BC - k_6 BC{\cdot}R + k_{-6} BCR - \delta_E BC \quad [3]$$

$$Dpp/Scw/\text{SBP/receptor}:\quad \frac{dBCR}{dt} = k_6 BC{\cdot}R + k_7 BR{\cdot}C - k_{-6} BCR - k_{-7} BCR - \delta_E BCR \quad [4]$$

$$\text{Dpp/Scw/receptor:}\quad \frac{dBR}{dt} = k_5 B{\cdot}R - k_{-5}BR + k_{-7}BCR - k_7 BR{\cdot}C - \delta_E BR. \qquad [5]$$

Here I, B, C, and R are the concentrations of Sog/Tsg, Dpp/Scw, SBP, and receptor, respectively, and IB, BC, BR, and BCR are the concentrations of the complexes. Multimeric receptor BMP complexes are not considered here. D_B is the diffusion constant for BMP; $\gamma_1 (V_{in}/V_{PV})\overline{DW}_{in}$ is the secretion rate of Dpp/Scw into the PV space after heterodimer formation. k_i and k_{-i} are the forward and reverse reaction rates, respectively; λTol is the cleavage rate of Sog by Tld. Λ, n, and K_h are the maximal production rate, the Hill coefficient, and the half maximal concentration, respectively, for the production of the SBP in response to BR. τ is the time lag associated with signaling, transcription, and production. BMPs are removed from the extracellular space by binding either to the binding protein or to the receptors and internalized with rate δ_E. The parameter values and additional information are given in *Supporting Materials* (section 5).

Results

First we analyze the local steady-state behavior of the signaling and feedback subsystems, treating the extracellular BMP (Dpp/Scw) as a parameter. (Hereafter we refer to Dpp/Scw as BMP.) Dimensionless forms of equations (Eqs. **2–5**) were solved numerically to obtain steady-state levels of SBP and complexes for different levels of extracellular BMP (22) (*Supporting Materials*, section 7.2). Positive feedback through SBPs leads to bistability at the level of BRs for certain choices of parameters; a typical result is shown in Fig. 1*e*. For low levels of BMP, the level of bound receptor BR (Dpp/Scw/Tkv/Sax) lies near the lower branch, which corresponds to equilibrium between the extracellular and receptor-bound BMP (dashed red line), with little contribution from the SBP. When BMP exceeds the critical value corresponding to the turning point on the lower solution branch, the steady state lies on the upper solution branch, where the BR is much greater than the binding equilibrium value. Because the local dynamics predict a bistable response when BMP is treated as a parameter, the existence of a switch point between adjacent cells in a BMP gradient is easy to understand. Those cells that detect a BMP level below the limit point adopt a fate on the lower branch, whereas those cells that detect a BMP level above the limit point adopt a fate on the upper branch, and this is precisely what happens in case 3 (*Supporting Material*, section 4.5). However, this mechanism is not sufficient to explain the contraction of the high-signaling region. Another possibility is that the state of the system depends on the history of the signal the cells receive over time, because some cells exposed to a sufficient signal reach the upper branch, whereas neighboring cells may return to the lower branch. As we show next, when positive feedback interactions are included in the extracellular BMP patterning model with endocytosis of BMP, the experimentally observed contraction emerges naturally.

Theoretical Predictions. When internalization is incorporated, the extracellular and receptor/SBP interactions are strongly coupled, because binding facilitates the removal of BMP from the PV space. Thus, the positive feedback affects not only the transient evolution of the extracellular BMP distribution but also the steady-state distribution. For simplicity, we suppose that receptors and binding proteins internalize at the same rate, but the general results are not dependent on this choice (D.M.U., unpublished data). Experimental evidence supports this constitutive internalization model (23).

To understand the interplay between the extracellular gradient and the intracellular positive feedback, the evolution equations (Eqs. **1–5** above and Eqs. **5–8** in *Supporting Materials*, section 3) were solved using zero initial conditions for all species except free receptors and Tld. The temporal evolution of extracellular Dpp/Scw and Dpp/Scw/Tkv/Sax is shown in Fig. 2 *a* and *b*. Initially, the extracellular Dpp/Scw and Dpp/Scw/Tkv/Sax profiles increase in tandem, reflecting a quasi-steady state in which the level of bound receptor is determined by a balance between the on- and off-rates of ligand and the degradation rate of Dpp/Scw/Tkv/Sax. After ≈30 min, the positive feedback loop enhances the level of BRs, thus also increasing the removal rate of BMP from the extracellular space. As peak signaling increases, the extracellular level of BMP decreases. During the transition phase, in which the initial smooth pattern of pMad expression evolves into a switch-like distribution, there is competition between the rate at which BMP is removed from the system and the rate of increased signaling facilitated by the positive feedback. Although many cells in the PV space are temporarily exposed to high levels of BMP signaling, only those that are exposed to a high signal for a sufficient duration reach the upper stable solution (Fig. 2*c*). The transient evolution of extracellular BMP and the BRs is noteworthy because the extracellular BMP profile grows initially, as in existing models with continuous BMP production (16, 17). However, after ≈30 min, the extracellular BMP profile decreases in amplitude throughout the PV

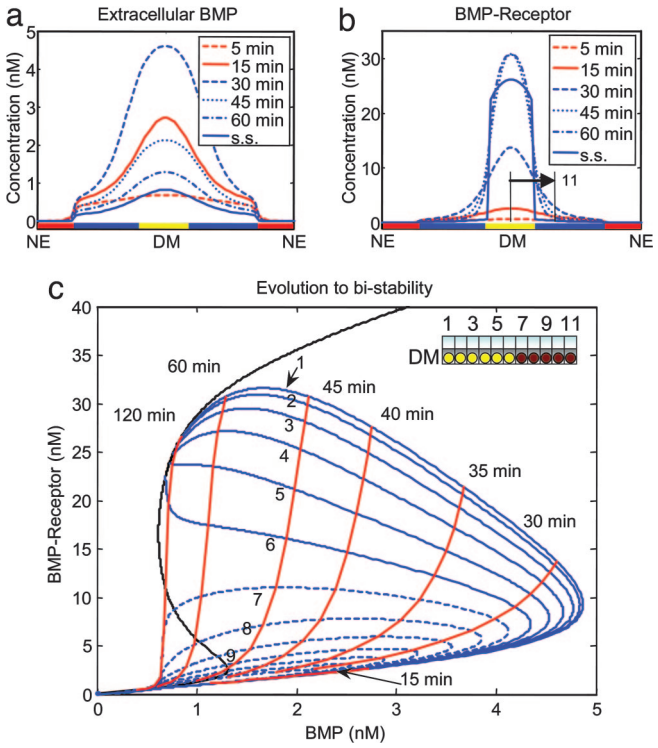

Fig. 2. Transient evolution of the full patterning model with positive feedback. (*a*) The concentration of extracellular BMP rises initially, reaches a peak at ≈30 min, and then begins to decrease in amplitude. (*b*) BR first produces a broad, low-level signal in ≈30 min and then rapidly contracts and increases in amplitude at the DM as the contribution from positive feedback increases. (*c*) The transient evolution to the switch-like spatial distribution of BR. The solid black line is the equilibrium curve as shown in Fig. 1*e*. Solid blue lines trace the temporal evolution of BMP and BR at a particular point in space. The labels on the orbits correspond to the numbering of the cells. The blue dashed lines correspond to cells for which the level of signaling first increases but then degradation removes BMP rapidly, causing them to return to the lower solution branch. The intersections of the solid red curves with the blue curves give the evolution at the indicated times.

DEVELOPMENTAL BIOLOGY

space, whereas the level of BMP bound to receptor continues to grow and sharpen. As time progresses, the spatial extent of BR contracts, but the peak level at the DM increases in amplitude, a feature not previously seen in other BMP patterning models (Fig. 2*b*). At steady state, the extracellular BMP distribution is very flat, whereas the level of BRs is a step function that corresponds well with the width of pMad expression and Dpp localization seen in late stage-5 embryos. Interestingly, there is a slight overshoot, because the maximum amplitude is slightly lower than at 60 min.

To further explicate the transient evolution of the spatial distribution, we show in Fig. 2*c* the evolution of the level of BMP and BR at different positions in the PV space that correspond to the location of different cells on the earlier equilibrium diagram (Fig. 1*e*). Cell number one corresponds to the cell adjacent to the DM, whereas cell number n is n cell widths away from the midline. The BMP vs. BR trajectories for all cells initially track the receptor-binding equilibrium line, and as the binding protein is produced, the level of BR increases. As the level of SBP increases, the rate of removal of BMP from the extracellular space also increases, and the BMP levels begin to decline. Those cells near the DM detect higher levels of BMP first and produce more SBP, which further increases the BR on these cells. Cells farther from the DM initially detect increasing BMP at levels greater than the limit point but are outcompeted by cells closest to the DM, and as BMP levels decline, the level of BR returns to the lower branch. Thus, although many cells are transiently exposed to high levels of BMP, only a small number of cells reach the upper stable branch due to limited levels of BMP. This finding is consistent with the local loss of signaling observed in embryos injected with activated *tkv*, which leads to a loss of signal (shadow) near the region of high signaling (9).

In patterning based on positive feedback as described here, the fate of cells is determined not only by a threshold of morphogen but also by the history of exposure to that morphogen. This finding suggests that the determination of a high- or low-signaling fate depends on the time integral of a rapidly changing extracellular morphogen, as was suggested earlier in other contexts (24, 25).

For the calculations reported here, the time lag is set to 0. Increasing the time lag slows the patterning process but also leads to a more pronounced contraction (*Supporting Materials*, section 4.8) and our analysis suggests that the time lag must be less than ≈10 min in order for dorsal surface patterning to occur within the developmental time window. This time is reasonable for transcription, translation, and postprocessing at this stage of development.

Robustness Results. Although heterodimer formation (1), limited diffusion length (17), and other upstream processes may be important for the robustness of the evolution of the extracellular morphogen profile, it is unclear how robustness is affected by the positive feedback loop that leads to an exposure response (1, 17). When surface-binding proteins are involved, the situation is more complex, but we can test the robustness of spatial patterning to extracellular perturbations of Sog, Tsg, Dpp, Scw, and Tld, and by perturbing the level of receptors, binding protein, and other factors.

Fig. 3 shows that the theoretical predictions for homozygous and heterozygous mutants produce phenotypes that correspond well with the observed embryonic phenotypes (Fig. 3 *a–c*) at 60 min. In this model, the $sog^{-/-}$ and $tsg^{-/-}$ profiles produce the same computed profile. However, it has been observed that less Dpp binds to the surface in *tsg* mutants than in *sog* mutants (9), which may result from Tsg aiding in the binding of BMP to receptors, which was not considered here. In Fig. 3*b*, the profile is robust with respect to changes in the levels of Tsg, Tld, and to a lesser degree, Sog as reported in ref. 16. It is also robust with respect to reductions in the

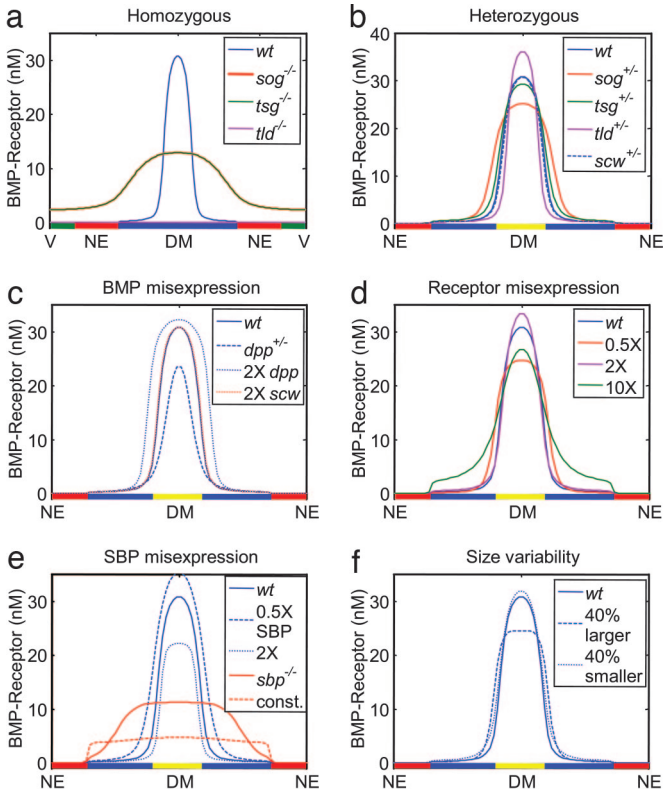

Fig. 3. Positive feedback and receptor-mediated degradation leads to morphogen distributions that correspond with the phenotypes for homozygous and heterozygous mutants. (*a*) Homozygous mutants for *sog*, *tsg*, and *tld*. The distribution of BR for the *tld* mutant leads to essentially zero signaling at 60 min. (*b*) Heterozygous *sog*, *tsg*, and *tld* mutants exhibit expected levels of robustness. (*c*) Heterozgyous and overexpressed *scw* leads to WT-like pattern, whereas the same is not true for *dpp*. (*d*) Patterning is resilient to changes in the levels of receptors. (*e*) Response to misexpression of SBP. (*f*) Patterning exhibits scale invariance for 40% increases or decreases in cross-sectional length of embryos.

level of Scw, but not Dpp, (Fig. 3*c*) principally as the result of heterodimer formation (*Supporting Materials*, section 2) (1). Furthermore, the spatial distribution of BRs is resilient to significant perturbations in the level of receptors (Fig. 3*d*) at 60 min. The positive feedback mechanism is insensitive to moderate changes in the level of SBP (Fig. 3*e*). However, it is sensitive to other perturbations, including knockout of SBPs, which leads to low-level BMP binding to receptors (Fig. 3*e*), consistent with the increased spatial extent of ligand–receptor interactions observed in Medea-null embryos (9). The system also exhibits a fair amount of scale invariance (Fig. 3*f*). General mechanisms that ensure scale invariance are known (26).

As mentioned earlier, significant alteration in Tkv expression has little effect on dorsal surface patterning. Zygotic knockout embryos exhibit WT-like distributions (Fig. 4*a*), injection of *tkv*+ mRNA into developing embryos results in either no change or a slight decrease in pMad signaling (9), and sufficient overexpression of Tkv also tends to decrease signaling amplitude but not the overall width (16). A reference case was chosen to measure the robustness of the system to changes in receptor level, which here is the BR distribution at 60 min for a receptor concentration of 320 nM. To investigate this robustness, we varied the level of receptors from 16 nM (≈120 receptors per cell) to 1.6×10^5 nM (≈1.2×10^6 receptors per cell) and normalized the profiles to the reference system. With positive feedback, we observed a slight decrease in BR for levels >320

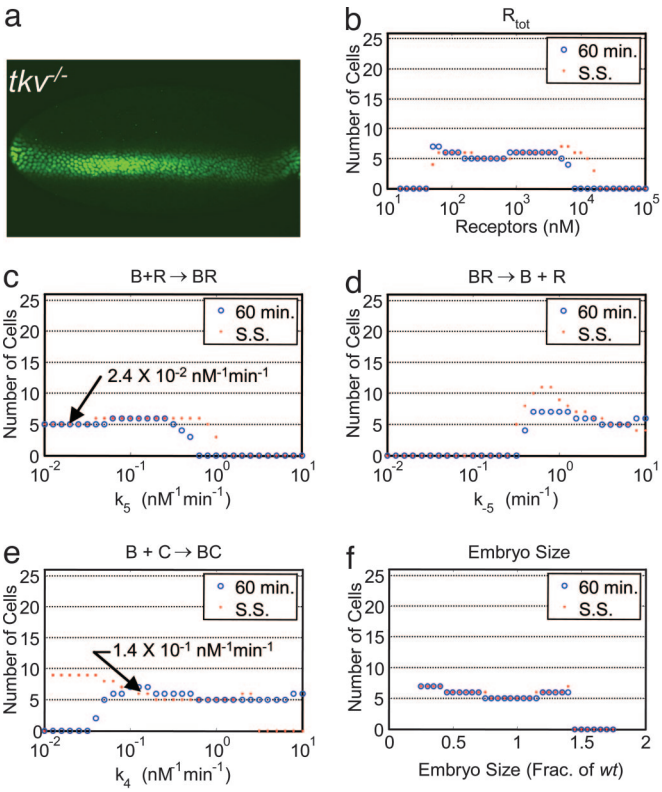

Fig. 4. Sensitivity of positive feedback to receptor levels and binding parameters. (*a*) *tkv* zygotic mutant embryo homozygous for the $tkv^{7-/-}$ allele exhibits WT pMad staining. (*b*) Robustness to specific level of receptors. The number of cells from the DM whose level of BR exceeds a threshold level of 50% of the reference system maximum 60 min. (○) and steady-state (●) is shown for receptor levels that vary from 16 nM to 1.6×10^5 nM. (*c* and *d*). Patterning is more sensitive to the on-rate (*c*) and off-rate (*d*) of BMP binding to receptor. (*e*) For proper patterning, the on-rate for SBP binding BMP is ≈6-fold greater than the on-rate for BMP binding receptor. (*f*) Patterning is essentially independent of the specific size of the embryo over a wide range of lengths.

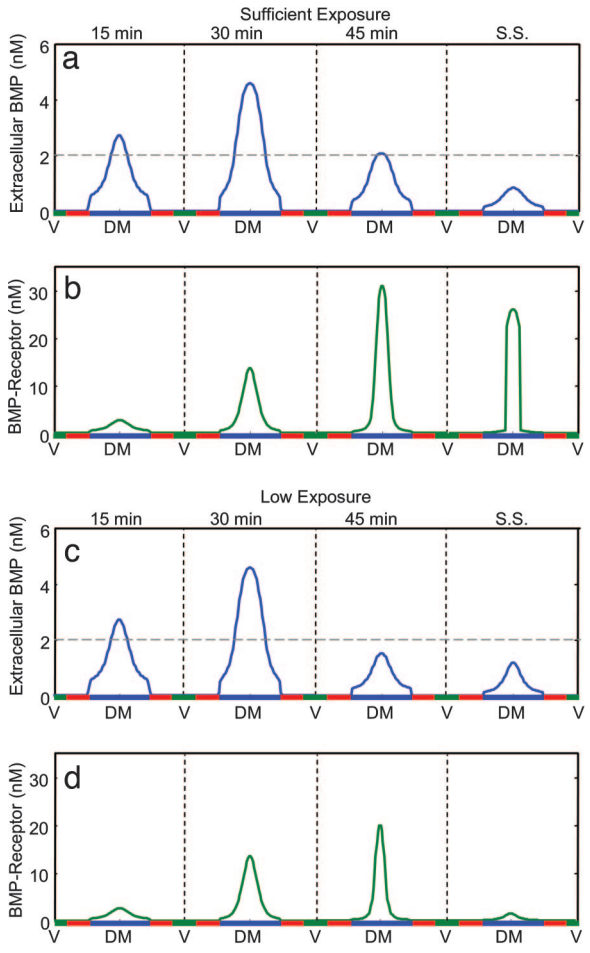

Fig. 5. Illustration of the mechanism for transient patterning with hysteresis. Transient evolution of extracellular BMP (*a*) and BR (*b*) leads to a spatial bistability and low extracellular levels of BMP at steady state. (*c*) The same as in *a* except the extracellular BMP levels drop more rapidly after the same initial 30 min of patterning imposed in this case by reducing the BMP input to 2% of WT. The steady-state levels of extracellular BMP in *a* and *c* are very similar. (*d*) However, due to the lower exposure of BMP over time, all cells return to the lower solution branch.

nM (Supporting Materials, section 7.2), consistent with either a loss or no change in the level of signaling in embryos with ectopic *tkv* (9, 16). However, although the amplitude varied, the overall width of signaling was very robust at both 60 min and at steady state (Fig. 4*b*) when measured by the number of cells greater than a threshold value of 50% of the maximum amplitude in the reference system. For this threshold, WT-like patterning is expected for receptor levels that vary from 5×10^1 nM to 6×10^3 nM at 60 min. (open blue circles) and which expands to $\approx 5 \times 10^1$ nM to 1.2×10^4 nM at steady state (solid red circles).

Patterning is more sensitive to the receptor and SBP forward-binding rates. In qualitative terms, positive feedback through SBP is only effective if the on-rate between free ligand and receptor is sufficiently low and the on-rate to the SBP is sufficiently high so that up-regulation of the SBP brings additional BMP into the vicinity of receptors (Fig. 4 *c* and *e*). Interestingly, the on-rate of a certain BMP, BMP2, to Cv-2 (a candidate SBP) is ≈6-fold higher than the on-rate of BMP2 to its type I receptor (1.4×10^{-1} and 2.4×10^{-2} $nM^{-1} \cdot min^{-1}$, respectively) (19, 27, 28). The model is also sensitive to the off-rate of BMP from the receptor (Fig. 4*d*) but less sensitive to the off-rate from the SBP (*Supporting Materials*, section 7.2). The width of high levels of BR is also insensitive to the size of the embryo (Fig. 4*f*).

Discussion

The dorsal/ventral patterning model formulated herein is based on the current understanding of the kinetic interactions between morphogens and inhibitors in the PV space and incorporates the effects of various dimeric forms of BMPs and their regulators on signal transduction. Our simulations show that the model can explain the observed localization of BMPs at the DM within the proper time scales, and it predicts that this can be achieved with nanomolar BMP concentrations, consistent with observations in cell culture (29). It also predicts the correct phenotypes for various homo- and heterozygous mutants, and it demonstrates significant robustness to changes in gene dosage of many components and in the size of the embryo.

An open problem in the interpretation of morphogen gradients is understanding how cells respond to a transiently evolving extracellular morphogen distribution (25). One possibility is that a steady-state gradient forms, and a time control cue is released to signal that cells should respond to that gradient according to their spatial position. Another idea is that the cellular state changes in response to the time-dependent morphogen distribution (25). The model described here, which incorporates both positive feedback and degradation/internalization of BMP, suggests a mechanism in which cells respond to a transient extracellular gradient by producing a factor that stabilizes signaling for cells that have been exposed to the ligand sufficiently, while

at the same time reducing the extracellular concentration of morphogen to reinforce the low-level signaling fate of adjacent cells. In this case, cells respond not only to the level but also to the time they are exposed to the extracellular signal (24, 30, 31). Initially the cellular response tracks the BMP gradient, but in later stages the positive feedback loop establishes a switch-like distribution of cells that have either a high- or low-signaling state. To illustrate this phenomenon, consider an evolving extracellular gradient that rises and falls before stabilizing at a steady-state distribution, as shown in Fig. 5*a*. The interpretation of the changing gradient (here the level of signaling receptors) is shown in Fig. 5*b*, in which two distinct regions are shown: a high-signaling region and a low-signaling region. Now suppose that exposure is limited by reducing BMP production after 35 min. The response is initially the same as before (compare Fig. 5 *b* and *d*), but due to the rapid decrease in morphogen, the response returns to a low-signaling state. The final distribution of morphogen is nearly the same in the two cases (compare Fig. 5 *a* and *c*), and the standard morphogen model would suggest that the output response would be the same, yet the history of the morphogen gradient is different, and this leads to steady-state responses that are very different.

The key to establishing such a system is the induction of a positive feedback component (9). Although the identity of the component that provides this function in the embryo is not yet known, we show here that a cell SBP such as Cv-2 can provide that activity. Cv-2 binds BMP molecules, is induced by positive feedback from BMP signaling, and at least one form binds to the surface (19). Remarkably, posterior cross-vein development uses a related set of extracellular modulators to achieve a similar spatial localization of BMP ligands. In that case, the ligands are Dpp and Gbb, and the modulators are Sog, the Tsg-related factor Cv, and the Tolloid-related factor Tlr (18). A major molecular difference between the posterior cross-vein pathway and signaling in the embryo is that the former also requires the extracellular protein Cv-2 (18). Cv-2 contains cysteine-rich domains related to those found in Sog as well as a partial Von Willebrand domain. Our recent data demonstrates that this protein not only binds Dpp and Gbb, but also binds to cell surfaces via the Von Willebrand domain and more importantly, its expression is induced by Dpp signaling (M.S., A. Ralston, S. Blair, and M.B.O., unpublished data). Although Cv-2 is required for promoting high-level BMP signaling in the cross-vein and during zebrafish gastrulation, its loss does not seem to affect early embryonic development (M.S. and M.B.O., unpublished data). Nevertheless, it serves to exemplify the type of molecule that could be involved in a positive feedback loop. There are several other CR-containing proteins in *Drosophila*, and numerous examples are found in vertebrate systems. In addition, the exact binding motif is likely to be unimportant. Other extracellular BMP-binding proteins such as the proteoglycan Dally (32), small leucine-rich proteoglycan family members such as Tsukushi (33), and the glycosylphosphatidylinositol-linked protein Dragon (34) could potentially act as positive feedback modulators of BMP signaling. Other possibilities include a molecule that modifies the affinity of the receptor through an intra- or extracellular mechanism. However, such a mechanism has to both enhance pMad signaling and lead to accumulation of Dpp on the surface. One additional observation of note is that Tsg has recently been suggested to facilitate binding of BMPs to the cell surface (9). Although we have been unable to find any enhanced association of BMPs with receptors in the presence of Tsg (M.S., O. Shimmi, and M.B.O., unpublished observations) it is possible that Tsg could mediate this effect through enhancement of binding of BMPs to one of these alternative cell surface BMP-binding proteins.

We thank Osamu Shimmi for helpful comments on the manuscript and the reviewers for thoughtful and thorough reviews. Research was funded in part by National Institutes of Health Grant GM29123 (to H.G.O.), National Science Foundation Grant DMS 0317372 (to H.G.O.), and Biotechnology Training Grant (to D.M.U.). M.B.O. is an Investigator with the Howard Hughes Medical Institute.

1. Shimmi, O., Umulis, D., Othmer, H. & O'Connor, M. B. (2005) *Cell* **120,** 873–886.
2. Padgett, R. W., St Johnston, R. D. & Gelbart, W. M. (1987) *Nature* **325,** 81–84.
3. Arora, K., Levine, M. S. & O'Connor, M. B. (1994) *Genes Dev.* **8,** 2588–2601.
4. Ferguson, E. L. & Anderson, K. V. (1992) *Cell* **71,** 451–461.
5. Wharton, K. A., Ray, R. P. & Gelbart, W. M. (1993) *Development (Cambridge, U.K.)* **117,** 807–822.
6. Ruberte, E., Marty, T., Nellen, D., Affolter, M. & Basler, K. (1995) *Cell* **80,** 889–897.
7. Letsou, A., Arora, K., Wrana, J. L., Simin, K., Twombly, V., Jamal, J., Staehling-Hampton, K., Hoffmann, F. M., Gelbart, W. M., Massague, J. *et al.* (1995) *Cell* **80,** 899–908.
8. Haerry, T. E., Khalsa, O., O'Connor, M. B. & Wharton, K. A. (1998) *Development (Cambridge, U.K.)* **125,** 3977–3987.
9. Wang, Y. C. & Ferguson, E. L. (2005) *Nature* **434,** 229–234.
10. Biehs, B., Francois, V. & Bier, E. (1996) *Genes Dev.* **10,** 2922–2934.
11. Decotto, E. & Ferguson, E. L. (2001) *Development (Cambridge, U.K.)* **128,** 3831–3841.
12. Oelgeschlager, M., Larrain, J., Geissert, D. & De Robertis, E. M. (2000) *Nature* **405,** 757–763.
13. Ross, J. J., Shimmi, O., Vilmos, P., Petryk, A., Kim, H., Gaudenz, K., Hermanson, S., Ekker, S. C., O'Connor, M. B. & Marsh, J. L. (2001) *Nature* **410,** 479–483.
14. Marques, G., Musacchio, M., Shimell, M. J., Wunnenberg-Stapleton, K., Cho, K. W. & O'Connor, M. B. (1997) *Cell* **91,** 417–426.
15. Srinivasan, S., Rashka, K. E. & Bier, E. (2002) *Dev. Cell* **2,** 91–101.
16. Mizutani, C. M., Nie, Q., Wan, F. Y., Zhang, Y. T., Vilmos, P., Sousa-Neves, R., Bier, E., Marsh, J. L. & Lander, A. D. (2005) *Dev. Cell* **8,** 915–924.
17. Eldar, A., Dorfman, R., Weiss, D., Ashe, H., Shilo, B. Z. & Barkai, N. (2002) *Nature* **419,** 304–308.
18. O'Connor, M., Umulis, D., Othmer, H. & Blair, S. S. (2006) *Development (Cambridge, U.K.)* **133,** 183–193.
19. Rentzsch, F., Zhang, J., Kramer, C., Sebald, W. & Hammerschmidt, M. (2006) *Development (Cambridge, U.K.)* **133,** 801–811.
20. Eldar, A., Rosin, D., Shilo, B. Z. & Barkai, N. (2003) *Dev. Cell* **5,** 635–646.
21. Ralston, A. & Blair, S. S. (2005) *Dev. Biol.* **280,** 187–200.
22. Dhooge, A., Govaerts, W. & Kuznetsov, Y. A. (2003) *ACM Transactions on Mathematical Software* **29,** 141–164.
23. Mitchell, H., Choudhury, A., Pagano, R. E. & Leof, E. B. (2004) *Mol. Biol. Cell* **15,** 4166–4178.
24. Dillon, R. & Othmer, H. G. (1999) *J. Theor. Biol.* **197,** 295–330.
25. Gurdon, J. B. & Bourillot, P. Y. (2001) *Nature* **413,** 797–803.
26. Othmer, H. G. & Pate, E. (1980) *Proc. Natl. Acad. Sci. USA* **77,** 4180–4184.
27. Greenwald, J., Groppe, J., Gray, P., Wiater, E., Kwiatkowski, W., Vale, W. & Choe, S. (2003) *Mol. Cell* **11,** 605–617.
28. Sebald, W., Nickel, J., Zhang, J. L. & Mueller, T. D. (2004) *Biol. Chem.* **385,** 697–710.
29. Shimmi, O. & O'Connor, M. B. (2003) *Development (Cambridge, U.K.)* **130,** 4673–4682.
30. Harfe, B. D., Scherz, P. J., Nissim, S., Tian, H., McMahon, A. P. & Tabin, C. J. (2004) *Cell* **118,** 517–528.
31. Pages, F. & Kerridge, S. (2000) *Trends Genet.* **16,** 40–44.
32. Fujise, M., Takeo, S., Kamimura, K., Matsuo, T., Aigaki, T., Izumi, S. & Nakato, H. (2003) *Development (Cambridge, U.K.)* **130,** 1515–1522.
33. Ohta, K., Lupo, G., Kuriyama, S., Keynes, R., Holt, C. E., Harris, W. A., Tanaka, H. & Ohnuma, S. (2004) *Dev. Cell* **7,** 347–358.
34. Babitt, J. L., Zhang, Y., Samad, T. A., Xia, Y., Tang, J., Campagna, J. A., Schneyer, A. L., Woolf, C. J. & Lin, H. Y. (2005) *J. Biol. Chem.* **280,** 29820–29827.